Development 123, 321-328
Printed in Great Britain © The Company of Biologists Limited 1996
DEV3332

Mutations affecting development of zebrafish digestive organs

Michael Pack, Lilliana Solnica-Krezel, Jarema Malicki, Stephan C. F. Neuhauss, Alexander F. Schier, Derek L. Stemple, Wolfgang Driever and Mark C. Fishman*

Cardiovascular Research Center, Massachusetts General Hospital, 149 13th Street, Charlestown, MA 02129, USA and Department of Medicine, Harvard Medical School, Boston, MA 02115, USA

*Author for correspondence

SUMMARY

The zebrafish gastrointestinal system matures in a manner akin to higher vertebrates. We describe nine mutations that perturb development of these organs. Normally, by the fourth day postfertilization the digestive organs are formed, the epithelial cells of the intestine are polarized and express digestive enzymes, the hepatocytes secrete bile, and the pancreatic islets and acini generate immunoreactive insulin and carboxypeptidase A, respectively. Seven mutations cause arrest of intestinal epithelial development after formation of the tube but before cell polarization is completed. These perturb different regions of the intestine. Six preferentially affect foregut, and one the hindgut. In one of the foregut mutations the esophagus does not form. Two mutations cause hepatic degeneration. The pancreas is affected in four mutants, all of which also perturb anterior intestine. The pancreatic exocrine cells are selectively affected in these four mutations. Exocrine precursor cells appear, as identified by *GATA-5* expression, but do not differentiate and acini do not form. The pancreatic islets are spared, and endocrine cells mature and synthesize insulin. These gastrointestinal mutations may be informative with regard to patterning and crucial lineage decisions during organogenesis, and may be relevant to diabetes, congenital dysmorphogenesis and disorders of cell proliferation.

Key words: gut, intestine, liver, pancreas, zebrafish

INTRODUCTION

The goal of this work is to identify genes that fashion the vertebrate gut and its derivative organs. We hope to identify signals that guide lineage assignment, promote region-specific tubular growth and budding, and maintain the differentiated state.

The principle cellular functions of the gut are the digestion and absorption of nutrients, the former dependent upon exocrine and the latter upon absorptive epithelial cells. These cells differ in specialized function between the anterior and posterior intestine. The hepatocytes of the liver are crucial for metabolism of a broad array of endogenous and exogenous substances and for excretion of bile. The pancreas is composed both of acini of exocrine cells, which secrete digestive enzymes such as lipases and peptidases, and the Islets of Langerhans, which secrete insulin and other peptide hormones.

The gut in higher vertebrates originates from the endodermal-lined anterior and posterior intestinal portals (AIP and PIP), which will give rise to the fore- and hindgut, respectively. Although the details of assembly vary among species, in general a continuous tube is generated from these pouches by endodermal growth and migration combined with ventral folding of the embryo (Lamers et al., 1987). The foregut becomes the esophagus, stomach, and duodenum. The hindgut becomes the distal large intestine, and the region in between, the midgut, becomes the intermediate zone of the small and large intestines. Growth of the gut is accommodated by looping and rotation as the absorptive surface is incresed by villus formation. The pancreas and liver originate as endodermal buds from the foregut.

During maturation of the intestine, the lining cells develop from a simple cuboidal to a polarized columnar epithelium composed of several distinctive cell types. Outside the basement membrane there is growth of connective tissue, blood vessels, lymphatics, and nerves. Epithelial buds from the foregut extend into the adjacent mesenchyme and generate the pancreas and liver.

The signals that guide these cell fate decisions and maintain the differentiated state are unknown. Explant experiments suggest that the competence of the AIP (Le Douarin et al., 1968; Sumiya, 1976) differs from the PIP (Sumiya, 1976) in that only the former can generate anterior gut derivatives, and does so only in the presence of an appropriate inductive signal. Precardiac mesoderm is necessary for the liver to develop from foregut endoderm (Le Douarin, 1975).

When the experiments reported here were initiated it was not clear how fruitful a genetic approach would be to a vertebrate organ system such as the gastrointestinal tract, because it develops relatively late and depends upon cascades of prior embryological decision-making. However, targeted mutation of known genes in mice has shown, for example, that absence of *IPF-1* blocks development of pancreas (Jonsson et al., 1994), loss of neuronal nitric oxide synthase causes hypertrophy of the stomach (Huang et al., 1993), and mice homozygous for a null mutation in *Bcl-2* show degeneration of intesti-

nal villi (Kamada et al., 1995). These phenotypes illustrate the potential power of genetics in dissecting the steps of organotypic decision-making, despite the inherent complexities of large multicellular tissue arrays.

MATERIALS AND METHODS

Fish, embryos and larvae

Fish were raised and handled as described by Westerfield (1993). Day 1 of development was considered to commence 24 hours after fertilization. The ENU mutagenesis screen is described in the accompanying paper (Driever et al., 1996). Progeny were screened for developmental defects involving the digestive organs on days 5 and 6 using a Wild M10 dissecting microscope. Complementation analyses were performed by pairwise matings between all members of groups assigned locus names, with the exception of *no relief*^{m264}, which was not complemented to *piebald*^{m497}. Three mutants (*m73, m140, m750*) were lost as a result of illness during the course of this screen, and are not available for further analysis.

Histology, immunocytochemistry and electron microscopy

Embryos and larvae were fixed in 4% paraformaldehyde, embedded in methacrylate (JB-4, Polysciences, Warrington PA) and 3-5 μm serial sections were stained with hematoxylin and eosin, or methylene blue-azure II. Labelling for glycogen was performed using periodic acid-Schiff staining with and without diastase. For immunocytochemistry, embryos and larvae were fixed in Bouin's and embedded in paraffin. Five μm serial sections were stained with a guinea pig anti-porcine insulin antibody (Linco, Eureka MO), 1:100, overnight at 4°C, or rabbit anti-bovine carboxypeptidase A antibody (Rockland Inc., Gilbertsville PA), 1:1000, overnight at 4°C. Texas red-conjugated goat anti-guinea pig and FITC-conjugated goat anti-rabbit antibodies (Jackson Immuno Research, West Grove, PA) were used as secondary antibodies, 1:100, for 2 hours at room temperature. For anti-cytokeratin staining, larvae and adult tissue were fixed in 4% paraformaldehyde, embedded in paraffin, sectioned, and treated with 0.2 mg/ml pronase XXV (Sigma) in PBS at 37°C for 30 minutes prior to application of the anti-cytokeratin antibody (AE1/AE3; Boehringer Mannheim) 1:100, 4°C overnight, followed by peroxidase-conjugated biotinylated goat anti-mouse secondary antibody (ABC Elite Kit; VectorLabs). For laminin imunostaining, rabbit anti-laminin antibody (Sigma) 1:200 was used at 4°C overnight, followed by a biotinylated goat anti-rabbit antibody (ABC Elite Kit, VectorLabs). For glucagon immunostaining, rabbit anti-glucagon antibody (generously provided by Dr Julia Polak, Royal Postgraduate Medical School, London, UK) was used 1:50, overnight at 4°C, followed by a FITC-conjugated goat anti-rabbit secondary antibody (Jackson Immuno Research, West Grove, PA.), 1:100 for 2 hours at room temperature.

Histochemical detection of leucine aminopeptidase, lipase and ATPase was accomplished using standard protocols (Bancroft and Stevens, 1990), as was alkaline phosphatase (Genius System, Boehringer Mannheim).

For electron microscopy, embryos and larvae were fixed in 2% glutaraldehyde for 1 hour at room temperature and postfixed in 1% osmium tetroxide, 1 hour, at 4°C. Specimens were dehydrated in ethanol, infiltrated with epoxy resin (Polysciences, Warrington PA), cut, mounted and stained following standard EM protocols and viewed with a Philips CM10 electron microscope.

Whole mount in situ hydridization was performed as described (Oxtoby and Jowett, 1993), using an anti-sense riboprobe generated from a full-length zebrafish *GATA-5* cDNA, a generous gift of Leonard Zon (Boston, MA), and were viewed and photographed using a Wild M10 dissecting microscope.

RESULTS

Zebrafish gastrointestinal tract development

The adult zebrafish digestive system is similar to that of other vertebrates (Fig. 1). The intestinal epithelium (Fig. 1A) includes most of the cell types observed in the small intestine of other vertebrates (absorptive, endocrine, goblet) but lacks crypts (Harder, 1975). Paneth cells have not been described in the fish intestine and an intestinal stem cell has not been identified in the teleost intestine, although there are differentiated proliferating cells in the base of the intestinal folds (Rombout et al., 1984). In *Cyprinids*, fat is absorbed in the proximal intestine and protein absorption occurs more distally (Rombout and Taverne-Thiele, 1984). A short terminal segment of the intestine is likely to be involved in ion transport and may be a homologue of the colon. As in other vertebrates, peristalsis is achieved by the contraction of an inner circular and outer longitudinal layer of smooth muscle, and is regulated by enteric nerves. The structure of the anterior end of the gut varies among vertebrates. As in all *Cyprinids*, the zebrafish is stomachless and the intestine is continuous with the pharynx through a short esophagus composed of a stratified squamous epithelium (Harder, 1975). The teleost liver (Fig. 1B)

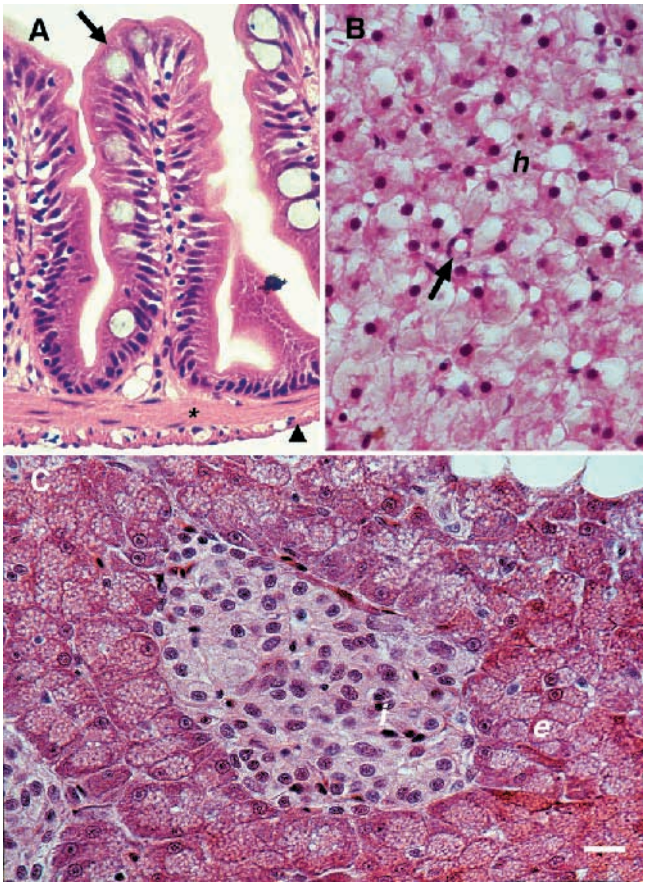

Fig. 1. Histology of adult zebrafish digestive organs. (A) Cross section of intestine. Arrow points to intestinal epithelium, arrowhead to outer longitudinal smooth muscle; * indicates inner circular smooth muscle. (B) Liver. Arrow points to intrahepatic bile duct. (C) Pancreas. e, exocrine cells; h, hepatocytes; i, islet. Scale bars, A, 25 μm; B and C, 15 μm.

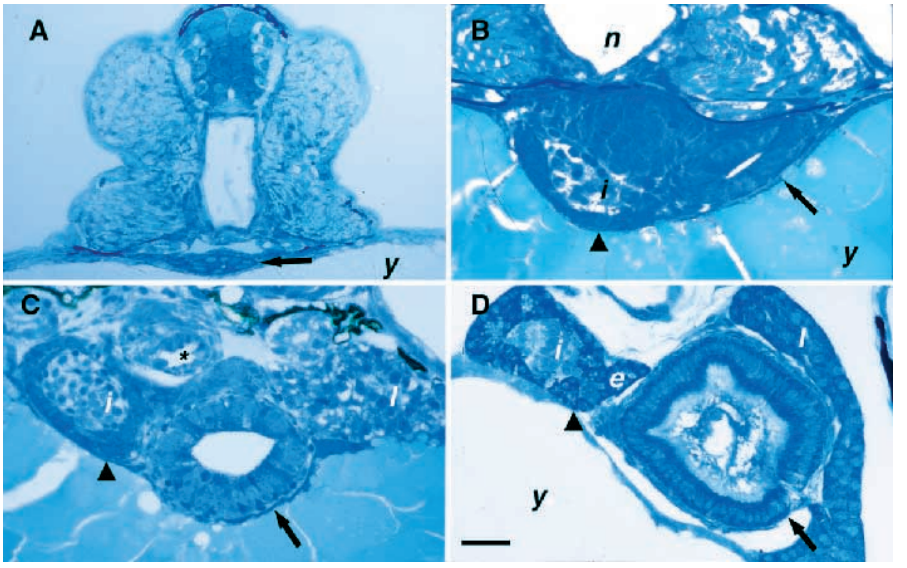

Fig. 2. Histology of the digestive organs in the developing zebrafish. Cross sections of proximal gut. (A) A small lumen is visible in the developing intestine (arrow) of the 36 hour postfertilization (hpf) embryo. (B) The intestine has enlarged (arrow) and the pancreatic islet (i) and exocrine precursor cells (arrowhead) are visible in the 52 hpf embryo. (C) The intestinal epithelium (arrow) has begun to polarize in the 72 hpf larvae. Exocrine precursors surround the islet (arrowhead). (D) The intestinal epithelium (arrow) has fully polarized and the pancreatic exocrine cells have differentiated (arrowhead) at 4 dpf. The liver is rostral to the plane of section in A and B. e, exocrine pancreas; i, pancreatic islet; l, liver; n, notochord; y, yolk; * labels pneumatic duct of gas bladder. Scale bars, A and D, 25 μm; B, 20 μm; C, 30 μm.

resembles that of the mammal but lacks a lobular architecture with portal tracts (Harder, 1975). The hepatocytes are arranged as cords of cells bathed in sinsuoidal portal blood. The intrahepatic bile ducts arise from bile cannaliculi and are scattered throughout the liver parenchyma. As in other vertebrates, a gall bladder is present for the storage of bile. The adult zebrafish pancreas (Fig. 1C) is a less coherent structure than that of the mammal in that several prominent islets are located near the proximal end of the pancreatic duct and accessory islets and exocrine tissue are scattered along the intestinal mesentery in close proximity to the pancreatic ducts (M. Pack, personal observation).

Fate maps of the zebrafish blastula indicate that endodermal precursors originate from marginal blastomeres, which involute early in gastrulation (Warga and Kimmel, 1990). As shown in Fig. 2A, at 36 hours postfertilization (hpf) the developing zebrafish gut is a cord of radially aligned cells. The anus and esophagus have not yet developed. By 52 hpf, as shown in Fig. 2B, a lumen is evident in the rostral gut, although not yet connected to the pharynx. By 72 hpf (Fig. 2C), differentiation is evident. Goblet cells have appeared and proximal intestinal cells have begun to polarize. The developing esophagus joins the proximal intestine to the pharynx. By 4 days postfertilization (dpf) the exocrine cells of the pancreas have

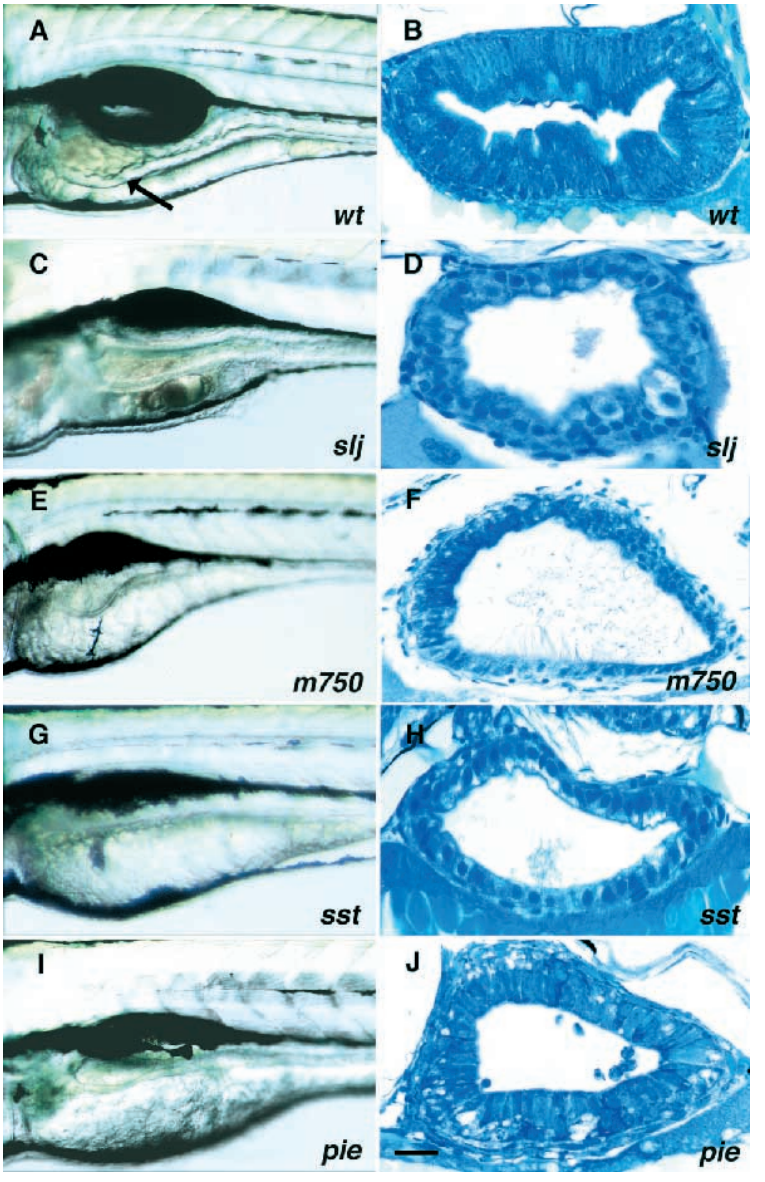

Fig. 3. Mutations affecting the developing zebrafish intestine. (A,C,E,G,I) Lateral views of living 5 dpf larvae. (B,D,F,H,J) Corresponding histological cross-sections through the mid-intestine. Lumen size varies with position along the anterior-posterior axis and with muscular contractions. (A,B) Wild type. The intestinal epithelium (arrow) is highly folded, bile is visible in the lumen and the gas bladder is inflated. The intestinal epithelium is polarized with basal nuclei and a microvillus brush border. (C,D) *slj* ^{m74}, (E,F) *m750*, (G,H) *sst*^{m311}, (I,J) *pie*^{m497}. The intestinal wall of all mutants is thin, lacks folds and the epithelium is not fully polarized and shows signs of degeneration. Scale bar, B, F and H, 20 μm; D, 15 μm; J, 25 μm.

differentiated, and the intestinal epithelium is polarized along its entire length and has a prominent microvillus brush border (Fig. 2D). Intestinal folds have developed in the rostral and mid-gut and peristaltic contractions are obvious. At 5 dpf proximal-distal regionalization is demonstrable by staining for lipase in the proximal and aminopeptidase in the distal epithelium (data not shown).

By Nomarski optics, liver cells and bile are visible by 3 dpf and hepatic blood flow by 4 dpf. Hepatocytes are evident histologically by 36 hpf, the extrahepatic biliary duct by 52 hpf, and endothelial-lined sinusoids at 3 dpf. The pancreas is visible using Nomarski optics at 4 dpf.

We have developed a series of molecular markers that characterize specific cell types of the zebrafish gut, liver, and pancreas and which have been helpful for mutant analysis. These are outlined in Table 1.

Mutations affecting digestive organs

The gastrointestinal tract is relatively obscured by overlying tissues. Peristalsis is slow and irregular, so cannot highlight defects as do contractions of the heart for the cardiovasculature. In addition, because the gut develops late relative to many developmental decisions, it is secondarily affected by mutations with effects elsewhere. We selected for further studies those with relatively gut-specific effects (Table 2).

Mutations that affect intestinal epithelium

Seven mutants affecting intestinal development were isolated. In six (examples of four mutants shown in Fig. 3), the intestinal tube develops without evident abnormality until 4 dpf. At this time the wild-type intestine (Fig. 3A,B) is folded and contains bile, and the epithelial cells are polarized and have a microvillus brush border. By contrast, in *slim jim (slj)* (Fig. 3C,D), *m750* (Fig. 3E,F), *straight shot (sst)* (Fig. 3G,H), *piebald (pie)* (Fig. 3I,J) and *no relief* (not shown), the intestinal epithelium is thin and lacks folds and the cells have only few scattered microvilli and lack evident polarization. In each of these mutants the intestinal epithelium begins to degenerate by 4-5 dpf.

Limitation of the defect to specific regions is a feature of several mutants. Anterior intestine is selectively perturbed in *slj*, posterior intestine is selectively affected in *meltdown (mlt)* and the esophagus in *m140* embryos. In *slj* mutants (Fig. 3C,D), despite the apparent lack of polarization of the anterior intestine, some cellular differentiation does occur. As shown by electron microscopy at 4 dpf, adherens and tight junctions are clearly visible between cells in the anterior intestinal epithelium of wild type (Fig. 4A,C) and *slj* (Fig. 4B,D). In *slj*

Table 1. Cell-specific markers for the digestive organs of zebrafish embryos and larvae

Marker	Cells
GATA-5	Hepatocytes, exocrine cells of pancreas, intestinal epithelium
Cytokeratin	Biliary cells of liver, ductular cells of pancreas, intestinal epithelium
Lipase	Intestinal epithelium (proximal)
Leucine aminopeptidase	Intestinal epithelium (mid-distal)
Insulin	Pancreatic islet
Glucagon	Pancreatic islet
Carboxypeptidase A	Exocrine cells of pancreas
Laminin	Basement membrane of intestine
ATP-ase	Intestinal epithelium, endothelial cells of liver sinusoids
Alkaline phosphatase	Intestinal epithelium

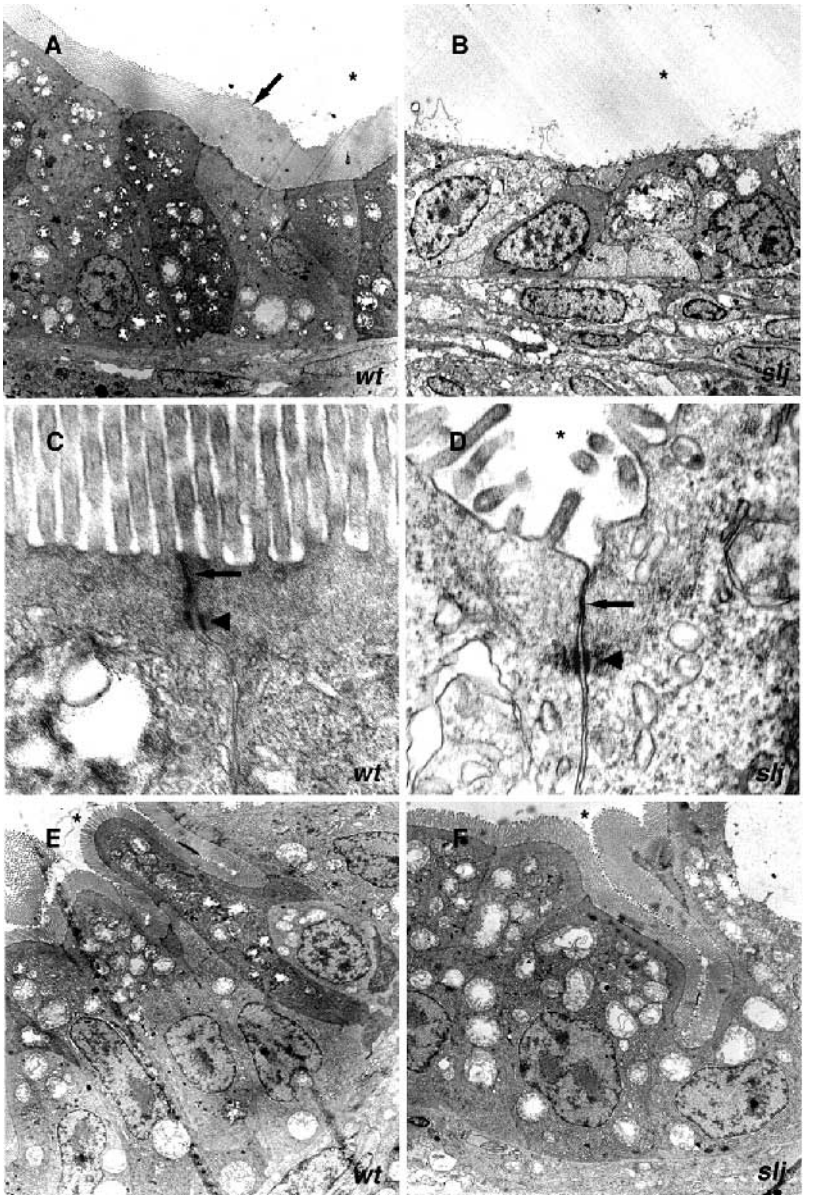

Fig. 4. Electron micrographs showing regional intestinal differentiation. (A,C,E) wild type and (B,D,F) slj^{m74}. (A) The wild-type anterior intestinal epithelium is columnar and has a prominent microvillus brush border (arrow). (B) slj^{m74} anterior intestinal epithelial cells are cuboidal with few microvilli. (C,D) Adherens (arrowhead) and tight junctions (arrow) are present in the anterior intestine of both (C) wild type and (D) slj^{m74}. (E,F) Posterior intestinal epithelium appears normal in both (E) wild type and (F) slj^{m74}. * labels the intestinal lumen. Magnification: A, ×950; B, ×1100; C, ×22,000; D, ×28,500; E, ×2200; F, ×2950.

Table 2. Mutations affecting the digestive organs

Genetic loci	Alleles	Phenotype	Other phenotypes
Group I: Foregut			
slim jim (slj)	*m74*	Intestinal epithelial degeneration (anterior), exocrine pancreas fails to develop	Reduced branchial arches (variable)
piebald (pie)	*m497*	Intestinal epithelial degeneration, exocrine pancreas fails to develop	
straight shot (sst)	*m311*	Intestinal epithelial degeneration, exocrine pancreas fails to develop	Reduced branchial arches
no relief (nor)	*m264*	Intestinal epithelial degeneration, exocrine pancreas fails to develop	Reduced branchial arches
-	*m750*	Intestinal epithelial degeneration, small exocrine pancreas	
-	*m140*	Esophagus fails to develop, degeneration of intestinal and pharyngeal epithelium	
Group II: Hindgut			
meltdown (mlt)	*m498*	Posterior intestine rendundant with expanded mesenchyme	
Group III: Liver			
beefeater (bef)	*m362*	Liver degeneration	
-	*m73*	Liver degeneration	Brain degeneration

these cells are also immunoreactive for a cytokeratin marker, the expression of which normally appears contemporaneously with polarization, and they have apical alkaline phosphatase activity (data not shown). The *slj* posterior intestinal epithelium is normal, even as assessed by electron microscopy (Fig. 4F; wild type, Fig. 4E). In *mlt*, however, the mid- and distal intestinal epithelium is disorganized and the mesenchyme expanded while the anterior intestine, liver and pancreas develop normally (Fig. 5). In *m140*, the pharynx, proximal intestine and liver begin to develop normally, but remain unconnected due to failure of esophageal development (Fig. 6). Subsequently the pharyngeal and intestinal epithelium degenerate.

In the four other intestinal mutants, epithelial degeneration occurs throughout the intestine. In one of these examined by electron microscopy, *pie* (Fig. 3I,J), the epithelial cells become polarized and develop adherens and tight junctions before degenerating (data not shown). In all mutations affecting the intestine, pronephric and mesonephric epithelium develop normally, indicating that the epithelial abnormality is limited to the gastrointestinal system.

Mutations that affect the liver

Two liver mutants were identified (Fig. 7). In *m73* mutants (Fig. 7C,D), reddish brown pigmentation accumulates in the liver. This is evident by Nomarski optics by 4 dpf, although histologically it appears by 2 dpf. Hepatocellular degeneration is evident by histology (Fig. 7D), and the abnormal liver pigmentation appears to be due to blood pooling around the degenerating hepatocytes. Development of the intra- and extra-hepatic bile ducts appears to be normal, as indicated by the presence of bile in the 4 dpf *m73* intestinal bulb and the presence of anti-cytokeratin immunoreactivity (data not shown). *m73* embryos also show brain degeneration. In humans, glycogen storage diseases are known to affect liver and brain. In the absence of feeding, glycogen is depleted from wild-type embryos by 6 dpf (Fig. 7G) but persists in the liver of *m73* embryos (Fig. 7H) at 6 dpf. This is compatible with impaired glycogen utilization in the *m73* liver. In the *beefeater (bef)* liver mutant (Fig. 7E,F) the histology resembles *m73*, but there is no brain degeneration.

Mutations that affect the pancreas

The relationship of the endocrine and exocrine lineages of the pancreas is uncertain. It has been proposed that they share a common precursor (Alpert et al., 1988; Teitelman et al., 1987; Gu et al., 1994; Guz et al., 1995), or that endocrine cells derive from the neural crest (Alpert et al., 1988). Therefore, it is of interest that four mutants develop islets in the essential absence of pacreatic acini.

Normally, the exocrine pancreas is first evident by the end of 3 dpf, a time which precedes overt intestinal differentiation, and appears fully developed by 4 dpf (Fig. 8A). In *slj* (Fig. 8B) and *pie* mutants, the islet is evident at 4 dpf, and expresses immunoreactive insulin (Fig. 8D) as does the wild type (Fig. 8C). *slj* islets are essentially devoid of surrounding cells (Fig. 8B), and the few there are lack zymogen granules. The exocrine cells of wild-type larvae at this stage express *GATA-*

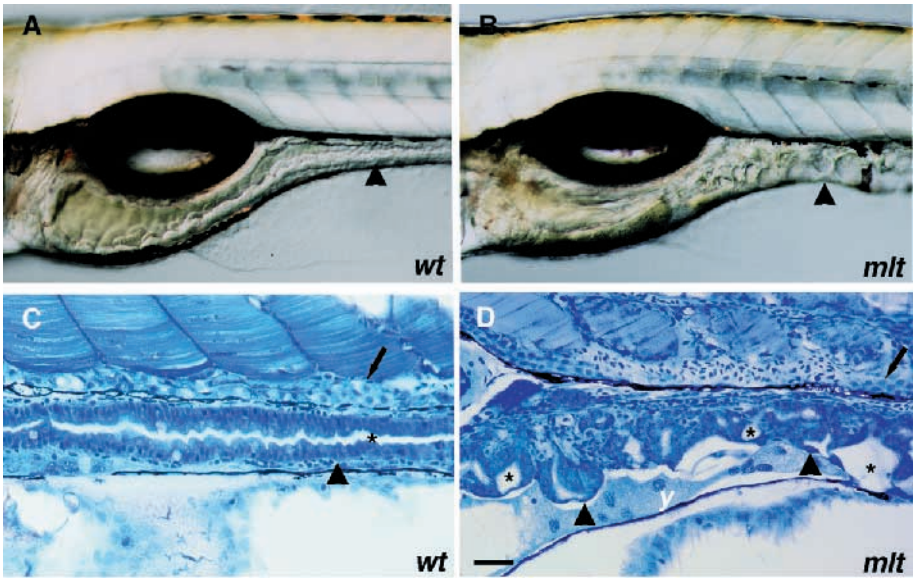

Fig. 5. *mlt*^{m498} perturbs posterior intestine. (A,C) Wild type, (B,D) *mel*. The posterior intestinal epithelium is disorganized and the mesenchyme expanded. * labels the intestinal lumen; arrowheads, posterior intestine; small arrows, pronephric duct. Scale bars, C and D, 30 μm.

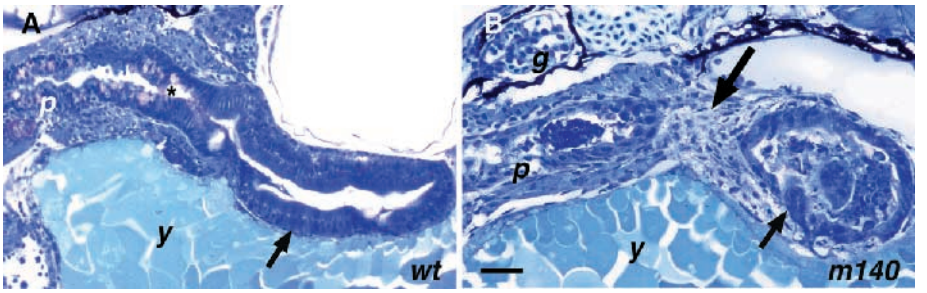

Fig. 6. In *m140* the esophagus fails to develop normally. (A) wild type, saggital section, 4 dpf. The intestine (arrow) is joined to the pharynx by the esophagus (*). (B) *m140*, 4 dpf. There is no connection (large arrow) between the intestine (small arrow) and pharynx, both of which have begun to degenerate. p, pharynx; g, glomerulus; y, yolk. Scale bars: A, 40 μm; B, 30 μm.

5 and immunoreactive carboxypeptidase A (Fig. 8E,G). In *slj*, carboxypeptidase A immunoreactivity is absent from the pancreas (Fig. 8F). This failure of exocrine cell development is also seen using a *GATA-5* probe, a marker of early gut development (Laverriere et al., 1994). Normally, all exocrine cells of the exocrine pancreas express *GATA-5* at 4 dpf (Fig. 8G). *slj* mutants lack *GATA-5* expression in this location (Fig. 8H) but retain it in other locations such as the heart, liver and intestine. However, at 3 dpf there is a normal pattern of *GATA-5* expression in the developing pancreas of all embryos of heterozygous *slj* matings. This suggests that in the *slj* pancreas there may be a transient population of exocrine precursors which do not survive. In *pie*, cellular exocrine differentiation seems to proceed further. Even though mature acini do not develop, a few cells express *GATA-5* and carboxypeptidase A in a ring around the islet at 4-5 dpf, in a pattern that resembles the 3 dpf islet. This selective failure of pancreatic exocrine development, with normal growth of islets, is also seen in *sst* and *nor* mutants. In *m750* embryos, the exocrine pancreas develops but is smaller than the wild type.

DISCUSSION

Screening for gastrointestinal mutations

We report here nine mutations that perturb gastrointestinal development. This is from a total of about 500 lines screened specifically for digestive organ defects at 5-6 dpf. It does not include mutations with generalized retardation or markedly pleotropic effects. The pancreas could not be identified reliably by this type of visual screen independently of the gut, but was involved in several foregut defects. Additional screens undoubtedly might enhance sensitivity by the use of lineage- or organ-specific markers. For example, cytokeratin and digestive enzyme markers distinguish the early stages of intestinal epithelial differentiation; the pancreatic exocrine cells express *GATA-5* and then carboxypeptidase; the pancreatic islets synthesize insulin and glucagon. Peristalsis can be rendered visible with dyes, and biliary excretion marked with phenol red (M. Pack, personal observation).

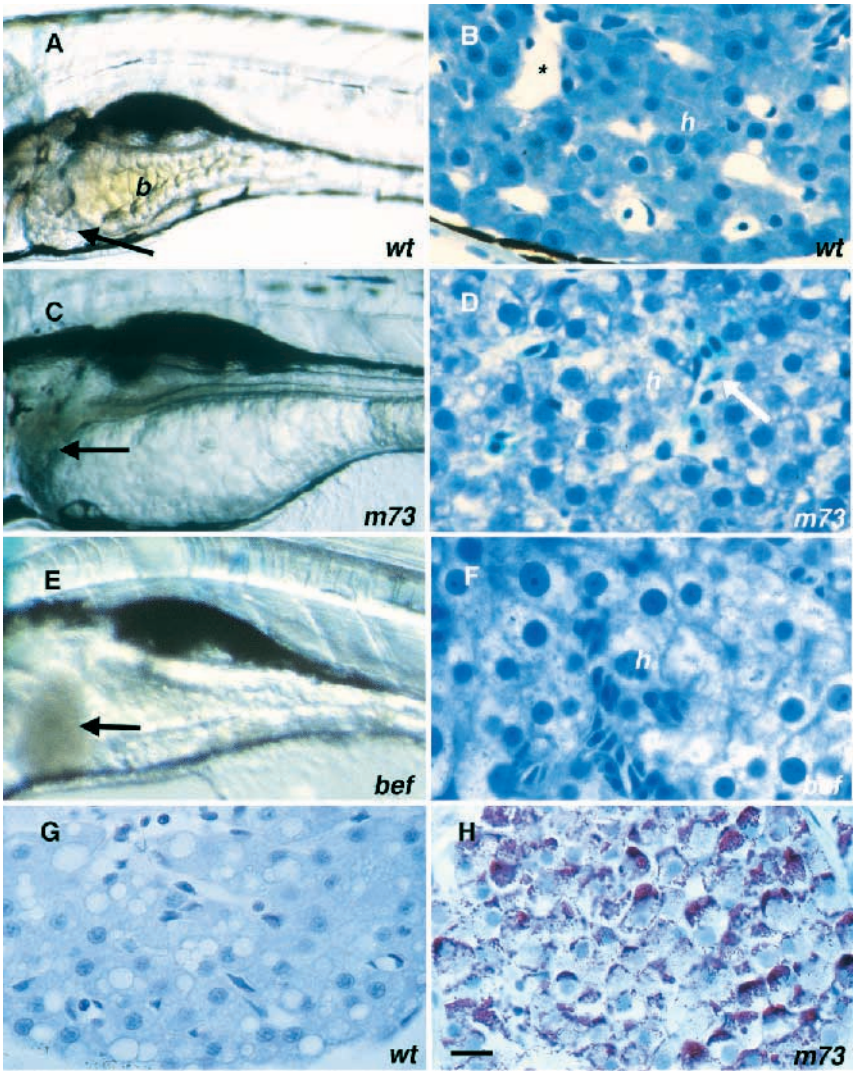

Fig. 7. Liver mutants. (A,BG) Wild type. (C,D,H) *m73*. (E,F) *bef* ^{m362}. (A) Lateral view of wild-type 5 dpf larva with bile (b) in intestinal lumen; arrow points to liver. (B) Cross section of wild-type liver 5 dpf with erythrocytes in the sinusoids (*) and hepatocytes (h). (C) The day-4 *m73* liver (arrow) has a gray-brown hue. (D) *m73* hepatocytes are degenerating and erythrocytes (arrow) are pooling in the sinusoids. (E) *bef*^{m362} liver (arrow) has a red-brown hue. (F) *bef*^{m362} hepatocytes also degenerate and compress the sinusoids. (G) Wild-type liver 6 dpf does not stain with PAS. (H) *m73* liver 6 dpf stains for PAS. Scale bar, 15 μm.

Patterning and differentiation

Specialization along the length of the gut characterizes all vertebrate digestive systems, and establishment of axial polarity is assumed to be a key component of its organogenesis, although it has been without molecular underpinning. Several mutations disrupt the early stages of gut development in a region-specific manner. *m140* prevents formation of the esophagus, of interest because poor development of this gut region is responsible for a set of congenital human disorders referred to as esophageal atresia, and because intestinal metaplasia in the esophagus, which is considered a forerunner of esophageal cancer, may result from disordered cell renewal in this organ. *slj* has a selective effect upon the anterior intestine and *mlt* upon the posterior intestine. These regions have their origins in the endoderm of the foregut and hindgut, respectively, and remain different in function throughout life. The molecular underpinning of this regionalization is unknown but several homeobox (Yokouchi et al., 1995; Gaunt et al., 1990; Geada et al., 1992) and forkhead (Monagan et al., 1993; Sasaki and Hogan, 1993) genes are expressed in the developing gut in a region-specific manner and have been proposed to play such patterning roles. *Xlhbox8* (the *Xenopus* IPF-1 homologue; Wright et al., 1988), has specifically been proposed in this regard for anterior gut.

The signals that regulate the differentiation, death, and renewal of gut epithelial cells are largely unknown. Perhaps because of the high rate of proliferation, gut epithelium is an affected site in mutations of *N-myc* (Stanton et al., 1992) and *Bcl-2* (Kamada et al., 1995), genes which affect the balance of cell proliferation and cell death. In explant culture, mesenchyme of developing gut induces epithelial development (reviewed in Haffen et al., 1987), and, in some cases, can cause a heterotopic epithelium to adopt a new fate concordant with that of the region from which the mesenchyme was derived (Haffen et al., 1987; Mizuno and Yasugi, 1990).

In *slj* and most of the other gut mutants, differentiation proceeds through the original stages of organotypic assembly, with enzyme synthesis and epithelial polarization, and thereafter the intestine begins to degenerate. One explanation could be that a requirement for trophic support is initiated after the onset of differentiation, and that elements of this process, which may result from epithelial-mesenchymal interactions, are perturbed by the mutations. Precursor and differentiated cells certainly may have different trophic dependencies. Along these lines, EGF receptor mutant mice can generate an intestine, but villus development is impaired and intestinal architecture becomes disorganized and degenerates soon after birth (Threadgill et al., 1995; Miettinen et al., 1995).

Lineage

The lineage relationship of pancreatic endocrine and exocrine cells is of especial interest, partly because there is no significant renewal of either cell type in the adult, which has important therapeutic implications for diabetes and chronic

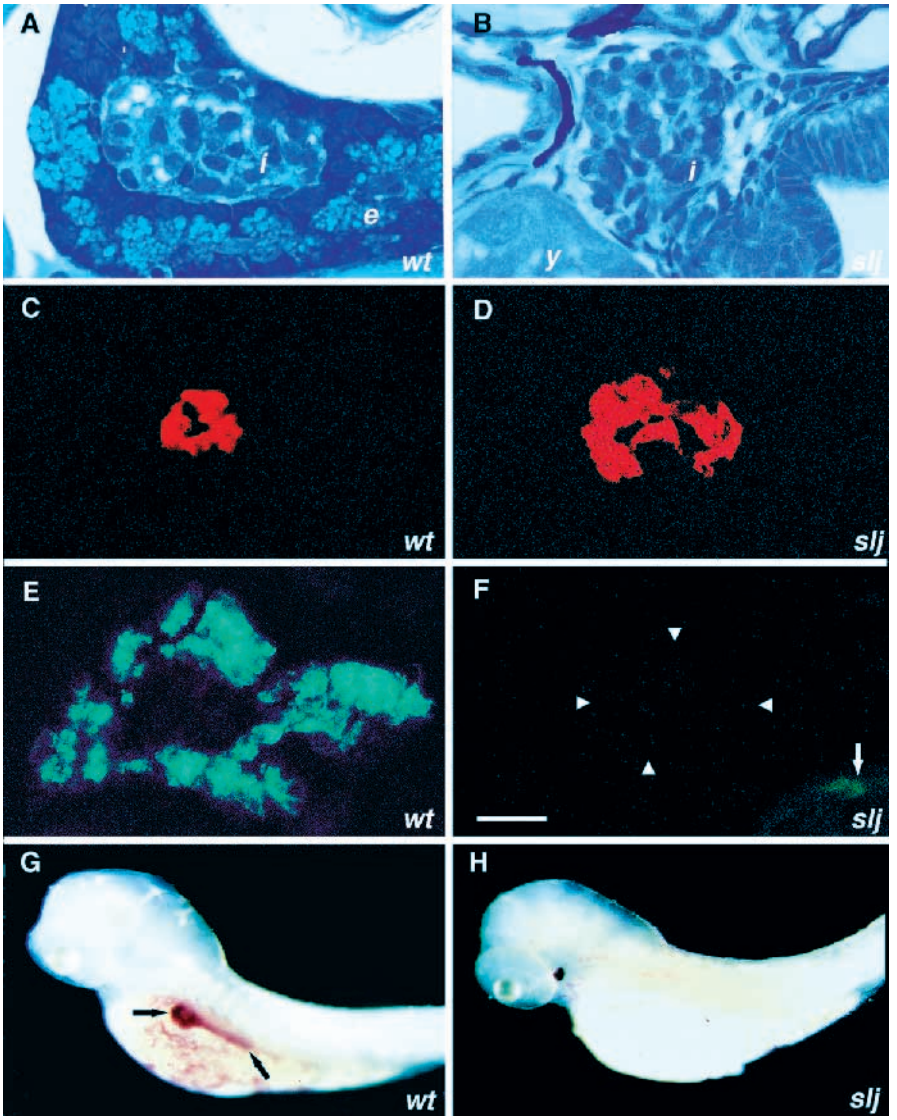

Fig. 8. Pancreas mutants. Pancreas development in (A,C,E,G) wild type and (B,D,F,H) *slj*^{m74} embryos. (A) Cross-section of the pancreas at 4 dpf showing islet (i) and exocrine (e) cells. (B) In *slj*^{m74} the islet appears normal but the exocrine cells have not developed. (C) Immunoreactive insulin in the wild-type islet. (D) Immunoreactive insulin in the *slj*^{m74} pancreas. (E) Immunoreactive carboxypeptidase A in the wild-type exocrine pancreas. (F) There is little if any immunoreactive carboxypeptidase A in the *slj* pancreas at 4 dpf. Arrrowheads mark the position of islet cells immunoreactive for insulin. Arrow, background staining in intestine. (G) *GATA-5* in situ hybridization in the wild type shows expression in the exocrine pancreas (arrows). (H) *slj*^{m74} does not express *GATA-5* in the exocrine pancreas. Scale bars, A,B,D and F, 15 μm; C,E, 20 μm.

pancreatitis. Whether there is a common precursor for the two cell types is controversial. Most cells express exocrine or endocrine markers alone, but recent reports suggest that there may be a few cells expressing both (Guz et al., 1995; Gu et al., 1994). The *IPF-1* gene may be a marker of the cells in the duodenum and pancreas with this bipotentiality (Guz et al., 1995). Compatible with this suggestion is the observation that, in the absence of the *IPF-1* gene, neither cell type is generated in the mouse. In *slj* mutants, islet cells can develop in the absence of differentiated pancreatic exocrine cells. It is possible that the *GATA-5*-expressing population, which transiently surrounds the developing islet at 3 dpf in mutants and wild type, represents an undifferentiated exocrine-endocrine precursor, one which could give rise to islet precursors before being lost by 4 dpf. Transplantation may help to determine whether the defect affects the exocrine cells in a cell-autonomous manner.

We thank Chris Simpson, Colleen Boggs and Margaret Boulos for outstanding technical help, John Lydon and Dennis Brown for invaluable assistance with electron microscopy, and Daniel K. Podolsky for advice and support. This work was supported by NIH RO1-HL49579 (M. C. F.), NIH RO1-HD29761 (W. D.) and a sponsored research agreement with Bristol Myers-Squibb (M. C. F. and W. D.). Support for M. P. came from in part from an NIH training grant to Dr Daniel K. Podolsky, and NIH K11-DK02157 (M. P.). Support for D. L. S. from the Helen Hay Whitney Foundation, for A. F. S. from Swiss National Science Foundation and EMBO, and for J. M. from Walter Winchell-Damon Runyon Cancer Research Fund.

REFERENCES

Alpert, S., Hanahan, D. and Teitelman, G. (1988). Hybrid insulin genes reveal a developmental lineage for pancreatic endocrine cells and imply a relationship with neurons. *Cell* **53**, 295-308.

Bancroft, A. and Stevens, A. (1990). Enzyme histochemistry: diagnostic applications. In *Theory and Practice of Histological Techniques* (ed. A. Bancroft J.D. and Stevens), pp. 401-412. New York: Churchill Livingstone.

Driever, W., Solnica-Krezel, L., Schier, A. F., Neuhauss, S. C. F., Malicki, J., Stemple, D. L., Stainier, D. Y. R., Zwartkruis, F., Abdelilah, S., Rangini, Z., Belak, J. and Boggs, C. (1996). A genetic screen for mutations affecting embryogenesis in zebrafish. *Development* **123**, 37-46.

Gaunt, S. J., Coletta, P. L., Pravtcheva, D. and Sharpe, P. T. (1990). Mouse *Hox-3.4* : Homeobox sequence and embryonic expression patterns compared with other members of the *Hox* gene network. *Development* **109,** 329-339.

Geada, A. M. C., Gaunt, S. J., Azzawi, M., Shimeld, S. M., Pearce, J. and Sharpe, P. T. (1992). Sequence and embryonic expression of the murine *Hox-3.5* gene. *Development* **116,** 497-506.

Gu, D., Lee, M. S., Krahl, T. and Sarvetnick, N. (1994). Transitional cells in the regenerating pancreas. *Development* **120**, 1873-1881.

Guz, Y., Montminy, M. R., Stein, R., Leonard, J., Gamer, L. W., Wright, C. V. and Teitelman, G. (1995). Expression of murine *STF-1*, a putative insulin gene trascription factor, in beta cells of pancreas, duodenal epithelium and pancreatic exocrine and endocrine progenitors during ontogeny. *Development* **121,** 11-18.

Haffen, K., Kedinger, M. and Simon-Assmann, P. (1987). Mesenchyme-dependent differentiation of epithelial progenitor cells in the gut. *J. Pediat. Gastroenterol. Nutrition* **6**, 14-23.

Harder, W. (1975). *Anatomy of Fishes*. Stuttgart: Eschweizerbartsche Verlagshuchhandlung.

Huang, P. L., Dawson, T. M., Bredt, D. S., Snyder, S. H., and Fishman, M. C. (1993). Targeted disruption of the neuronal nitric oxide synthase gene. *Cell* **75**, 1273-1286.

Jonsson, J., Carlsson, L., Edlund, T. and Edlund H. (1994). Insulin-promoter-factor-1 is required for pancreas development in mice. *Nature* **371**, 606-609.

Kamada, S., Shimono, A., Shinto, Y., Tsujimura, T., Takahashi, T., Noda, T., Kitamura, Y., Kondoh, H. and Tsujimoto, Y. (1995). *Bcl-2* Deficiency in mice leads to pleiotropic abnormalities: Accelerated lymphoid cell death in the thymus and spleen, polycystic kidney, hair hypopigmentation, and distorted small intestine. *Cancer Res.* **55**, 354-359.

Lamers, W. H., Spliet, W. G. M. and Langemeyer, R. A. T. M. (1987). The lining of the gut in the developing rat embryo. *Anat. Embryol.* **176**, 259-265.

Laverriere, A. C., MacNeill, C., Mueller, C., Poelmann, R. E., Burch, J. B. and Evans, T. (1994). *GATA-4/5/6*, a subfamily of three transcription factors transcribed in developing heart and gut. *J. Biol. Chem.* **269**, 23177-23184.

Le Douarin, N. M. (1975). An experimental analysis of liver development. *Medical Biol.* **53**, 427-455.

Le Douarin, N., Bussonnet C. and Chaumont F. (1968). Etude des capacites de differenciation et du role morphogene de l'endoderme pharygien chez l'embryon d'oiseau. *Ann. Embryol. Morphol.* **1**, 29-39.

Miettinen, P. J., Berger, J. E., Meneses, J., Phung, Y., Pedersen, R. A., Werb, A. and Derynck, R. (1995). Epithelial immaturity and multiorgan failure in mice lacking epidermal growth factor receptor. *Nature***376**, 337-341.

Mizuno, T. and Yasugi, S. (1990). Susceptibility of epithelia to directive influences of mesenchymes during organogenesis: Uncoupling of morphogenesis and cytodifferentiation. *Cell Diff. Dev.* **31**, 151-159.

Monagan, A. P., Kaestner, K. H., Grau, E. and Schutz, G. (1993). Postimplantation expression patterns indicate a role for the mouse forkhead/*HNF-3*α, β and γ genes in determination of the definitive endoderm, chordamesoderm and neuroectoderm. *Development* **119**, 567-578.

Oxtoby, E. and Jowett, T. (1993). Cloning of the zebrafish *Krox-20* gene *(Krx-20)* and its expression during hindbrain development. *Nucl. Acids Res.* **21,** 1087-1095.

Rombout, J. H. W. M., Stroband, H. W. J., and Taverne-Thiele, J. J. (1984). Proliferation and differentiation of intestinal epithelial cells during development of *Barbus conchonius* (Teleostei, Cyprindae). *Cell Tisse Res.* 207-216.

Rombout, J. H. W. M. and Taverne-Thiele, J. J. (1984). An immunocytochemical and electron-microscopical study of endocrine cells in the gut and pancreas of a stomachless teleost fish, *Barbus conchonius* (Cyprinidae). *Cell Tiss. Res.* **227**, 577-593.

Sasaki, H. and Hogan, B. L. (1993). Differential expression of multiple forkhead related genes during gastrulation and axial pattern formation in the mouse embryo. *Development* **118**, 47-59.

Stanton, B. R., Perkins, A. S., Tessarollo, L., Sassoon, D. A. and Parada, L. F. (1992). Loss of N-*myc* function results in embryonic lethality and failure of the epithelial component of the embryo to develop. *Genes Dev.* **6**, 2235-2247.

Sumiya, M. (1976). Differentiation of the digestive tract epithelium of the chick embryo cultured in vitro enveloped in a fragment of the vitellin membrane, in the absence of mesenchyme. *Wilhelm Roux's Arch. Dev. Biol.* **179**, 1-17.

Teitelman, G., Lee, J. K., and Alpert, S. (1987). Expression of cell type-specific markers during pancreatic development in the mouse: implications for pancreatic cell lineages. *Cell Tiss. Res.* **250**, 435-39.

Threadgill, D. W., Dlugosz, A. A., Hansen. L. A., Tennenbaum, T., Ulrike, L., Yee, D., LaMantia, C., Mourton, T., Herrup, T., Harris, R. C., Barnard, J. A., Yuspa, S. H., Coffey, R. J. and Magnuson, T. (1995). Targeted disruption of mouse EGF receptor: Effect of genetic background on mutant phenotype. *Science* **269**, 230-234.

Warga, R. M. and Kimmel, C. B. (1990). Cell movements during epiboly and gastrulation in zebrafish. *Development* **108**, 569-580.

Westerfield, M. (1993). *The Zebrafish Book*. Eugene, OR.: University of Oregon press.

Wright, C. V. E., Schnegelsberg, P. and De Robertis, E. M. (1988). *XlHbox 8*: a novel *Xenopus* homeo protein restricted to a narrow band of endoderm. *Development***104,** 787-794.

Yokouchi, Y., Sakiyama, J. I. and Kuroiwa, A. (1995). Coordinated expression of *Abd-B* subfamily genes of the *HoxA* cluster in the developing digestive tract of chick embryo. *Dev. Biol.* **169**, 76-89.

(Accepted 28 November 1995)